

# Enhancing Spatial Reasoning in Multimodal Large Language Models through Reasoning-based Segmentation

Zhenhua Ning<sup>1,2,3†\*</sup> Zhuotao Tian<sup>1\*</sup> Shaoshuai Shi<sup>4</sup> Guangming Lu<sup>1</sup> Daojing He<sup>1</sup>  
Wenjie Pei<sup>1,2✉</sup> Li Jiang<sup>3✉</sup>

<sup>1</sup>Harbin Institute of Technology, Shenzhen <sup>2</sup>Pengcheng Laboratory

<sup>3</sup>The Chinese University of Hong Kong, Shenzhen <sup>4</sup>Voyager Research, Didi Chuxing

wenjiecoder@outlook.com jiangli@cuhk.edu.cn

## Abstract

*Recent advances in point cloud perception have demonstrated remarkable progress in scene understanding through vision-language alignment leveraging large language models (LLMs). However, existing methods may still encounter challenges in handling complex instructions that require accurate spatial reasoning, even if the 3D point cloud data provides detailed spatial cues such as size and position for identifying the targets. To tackle this issue, we propose Relevant Reasoning Segmentation (R<sup>2</sup>S), a reasoning-based segmentation framework. The framework emulates human cognitive processes by decomposing spatial reasoning into two sequential stages: first identifying relevant elements, then processing instructions guided by their associated visual priors. Furthermore, acknowledging the inadequacy of existing datasets in complex reasoning tasks, we introduce 3D ReasonSeg, a reasoning-based segmentation dataset comprising 25,185 training samples and 3,966 validation samples with precise annotations. Both quantitative and qualitative experiments demonstrate that the R<sup>2</sup>S and 3D ReasonSeg effectively endow 3D point cloud perception with stronger spatial reasoning capabilities, and we hope that they can serve as a new baseline and benchmark for future work.*

## 1. Introduction

In recent years, multi-modal large language models (MLLMs) [1, 29, 49, 55, 56, 61] have managed to connect language and vision, bringing in a new era of artificial intelligence. These models have shown unprecedented abilities, enabling various fields to understand and create textual and

visual content, such as human-computer interaction, multi-media understanding, embodied intelligence, and more.

Building upon these foundations, recent developments in MLLMs have led to the emergence of 3D MLLMs [6, 18, 19, 48, 50], which demonstrate remarkable capabilities in 3D point cloud perception through enhanced vision-language alignment. Despite these achievements, current 3D MLLM-based approaches exhibit limitations in processing instructions that require sophisticated spatial reasoning. As shown in Fig. 1, the baseline model fails to accurately localize the target object. This observation raises an important question: while 3D point clouds inherently contain richer spatial information (e.g., precise measurements of size and position) compared to 2D images, why do models still struggle to effectively leverage these geometric properties? We posit that the development of robust spatial reasoning capabilities requires two critical components: an explicit reasoning mechanism and a dataset that encompasses complex reasoning scenarios.

In this work, we introduce the Relevant Reasoning Segmentation (R<sup>2</sup>S), a reasoning-based segmentation framework that enhances the spatial reasoning capabilities of 3D MLLMs through two key steps: 1) Reasoning Prior Learning and 2) Prior-guided Refinement. In the first step, the model is trained to generate spatial priors by identifying target-relevant objects, providing essential contextual information. In the second step, the model leverages these reasoning priors to refine hidden representations, facilitating precise target localization. In other words, the two steps emulate human reasoning behavior, *i.e.*, initially identifying relevant elements broadly and then scrutinizing them closely to pinpoint the target.

Analysis of existing datasets reveals that instructions requiring reasoning are often oversimplified and ambiguous, as illustrated in Fig. 5. This limitation constrains the training and evaluation processes for developing reasoning capabilities in 3D MLLMs. To address this limitation,

<sup>†</sup>Research Assistant at CUHKSZ.

<sup>\*</sup>Equal contribution to this work. <sup>✉</sup> Corresponding author.

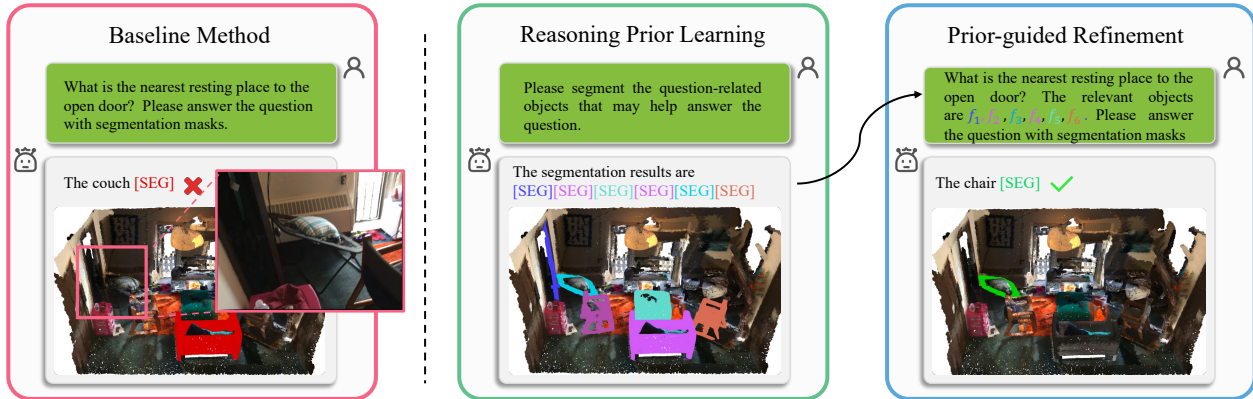


Figure 1. In contrast to the baseline model in Sec. 3.1, we introduce Relevant Reasoning Segmentation to explicitly guide the model’s reasoning by emphasizing target-relevant objects. In this instance, the object identified as the nearest resting place to the open door should be the chair marked by the red rectangle. The first to third columns in the image represent the prediction from the base method, the outcomes of reasoning prior learning, and the final prediction following prior guided refinement.

we present 3D ReasonSeg, a reasoning-based segmentation dataset that focuses on object functionality, visual attributes, and spatial relationships. The dataset comprises 25,185 training samples and 3,966 validation samples, with quality assurance maintained through manual verification processes. This dataset facilitates enhancement and comprehensive assessment of spatial reasoning capabilities.

Both our proposed R<sup>2</sup>S framework and the 3D ReasonSeg dataset contribute to substantial performance improvements on established benchmarks, demonstrating their complementary effects in enhancing spatial reasoning capabilities. In summary, our main contributions are:

- We propose the Relevant Segmentation (R<sup>2</sup>S), a reasoning-based segmentation framework that enhances spatial reasoning capabilities of 3D MLLMs by emulating human reasoning processes through two key components: Reasoning Prior Learning and Prior-guided Refinement.
- We propose 3D ReasonSeg, a reasoning-based segmentation dataset that focuses on object functionality, visual attributes, and spatial relationships, designed to enhance and comprehensively assess the spatial reasoning capabilities in 3D MLLMs.
- Extensive experimental results demonstrate that our R<sup>2</sup>S framework, combined with the 3D ReasonSeg dataset, achieves significant improvements in spatial reasoning across multiple benchmarks.

## 2. Related Work

### 2.1. 3D Scene Understanding

3D scene understanding requires models to detect objects and comprehend their characteristics in 3D space [3, 7, 8, 25, 33, 40]. Among these tasks, 3D segmentation

presents unique challenges as it demands point-wise classification within point clouds. Recent studies demonstrate that language integration enhances model performance, as evidenced in 3D Question Answering and 3D Referring tasks [2, 4, 21, 32, 58]. These language-guided tasks, which require models to respond to instructions or identify objects based on descriptions, underscore the importance of language comprehension and spatial reasoning capabilities.

The integration of language has supported models in transitioning from closed-set to open-set scenarios, such as in 3D Open Vocabulary Segmentation [4, 12, 14, 38, 41]. This step is critical as it allows the model to break free from being constrained by the finite set of categories in the training dataset. While most task-oriented studies focus on specific objectives, recent advancements in 3D multi-modal large language models have enabled addressing multiple 3D downstream tasks using these models [6, 20]. Furthermore, the assistance of 3D multi-modal large language models has empowered models to tackle more intricate object localization tasks [9, 60].

These prior studies have not adequately addressed the complex spatial reasoning capabilities required for comprehensive understanding of 3D scenes. In this work, we introduce Relevant Reasoning Segmentation and 3D ReasonSeg to address complex spatial reasoning challenges.

### 2.2. 3D Multi-modal Large Language Model

Significant progress has been made in the realm of 3D multi-modal large language models (3D MLLMs). Initial endeavors have predominantly concentrated on point clouds at the object level [16, 17, 30, 50], posing challenges in tackling complex tasks at the scene level. Recently, researchers have shifted attention to understanding entire scene point clouds [6, 18, 19, 48], significantly ad-

vancing 3D scene understanding.

Drawing from these advances, we present an efficient framework that handles various scene understanding tasks, with particular strength in segmentation. While existing 3D MLLMs can process basic spatial relationships, they struggle with complex spatial reasoning tasks. Our model, however, demonstrates superior performance in handling sophisticated spatial reasoning challenges.

### 3. Method

Efforts such as those outlined in [6, 18, 19] were dedicated to leveraging 3D MLLMs for a deeper comprehension of 3D point clouds. Nevertheless, it is evident that current methods encounter challenges in effectively managing intricate spatial relationships. Specifically, as illustrated in Fig. 2, while the model can accurately identify "What is the object that is used for sitting?", it struggles with queries such as "What is the object that is used for sitting and located near the desk with a monitor on it?"

To tackle this issue, in this work, we instruct the model to generate reasoning priors by paying attention to objects relevant to the target. Subsequently, the model examines the scene and these relevant objects more closely to locate the final target. We refer to this process as Relevant Reasoning Segmentation (R<sup>2</sup>S).

The remainder of this section is organized as follows: Sec. 3.1 introduces our baseline model, which demonstrates strong dense perception capabilities on 3D point cloud data. Sec. 3.2 elaborates on our proposed Relevant Reasoning Segmentation framework. Sec. 3.3 details the construction of our 3D ReasonSeg dataset, and Sec. 3.4 describes the comprehensive training pipeline.

#### 3.1. Baseline Model

Our baseline architecture consists of a multi-modal large language model (MLLM) and a Segmentation Head. Following [26], we extend the MLLM’s vocabulary with a special token [SEG] that instructs the Segmentation Head to generate corresponding segmentation mask. This design enables the MLLM to effectively perform fine-grained segmentation tasks while maintaining its core language understanding capabilities.

**Multi-modal Large Language Model.** There are three key components in the adopted MLLM for feature extraction: a visual encoder, a Q-Former, and a large language model (LLM). Initially, the point cloud  $X_p$  is processed through the visual encoder to extract dense features. To optimize computational efficiency, we employ super-point [28] within the visual backbone, aggregating the dense visual features into super-point features  $f_p$  to reduce the following computational burden. Subsequently, the Q-Former [29] compresses the scene’s information into several latent queries  $q_l$  based on the super-point features

$f_p$  and text embedding  $w$  of the instruction. After that, the latent queries  $q_l$  will serve as the visual input, along with the text embedding  $w$ , to be processed by the large language model  $\mathcal{F}_{LLM}$ . This process is formulated as:

$$f_p = \mathcal{F}_{enc}(X_p), \quad \hat{q}_l = \mathcal{F}_Q(q_l, w, f_p). \quad (1)$$

$$y_{txt} = \mathcal{F}_{LLM}(\hat{q}_l, w). \quad (2)$$

Inside the Q-Former  $\mathcal{F}_Q$ ,  $q_l$  is concatenated with  $w$  to be the query in both the self-attention and cross-attention layers of  $\mathcal{F}_Q$ , while  $f_p$  serves as the key and value in the cross-attention layer:

$$q_l, w = \text{SelfAttn}(\text{Concat}(q_l, w)), \quad (3)$$

$$q_l, w = \text{CrossAttn}(\text{Concat}(q_l, w), f_p, f_p). \quad (4)$$

**Segmentation Head.** If the output of LLM, *i.e.*,  $y_{txt}$ , contains [SEG] tokens, it means that the current query requires segmentation predictions. Then, the corresponding hidden features of the [SEG] token, *i.e.*,  $h_{seg}$ , are processed by the segmentation head  $\mathcal{F}_{dec}$  that follows the decoder structure of [24] to yield the requisite segmentation mask  $M$ , based on the reasoning between  $h_{seg}$  and  $f_p$ . The process can be formulated as follows.

$$M = \mathcal{F}_{dec}(h_{seg}, f_p). \quad (5)$$

The aforementioned framework seamlessly incorporates dense visual perception abilities into the output of the language model, allowing for the fusion of linguistic and visual information processing.

#### 3.2. Relevant Reasoning Segmentation

The baseline model can decently handle point cloud perception tasks. However, in our observations, the direct instruction tuning performed in [26] did not consider the spatial relationships among objects in the scene, hindering complex spatial reasoning, as illustrated in Fig. 8. Hence, to address this issue, we suggest that the model initially identifies the objects related to the target and their spatial relationships, serving as the reasoning prior to guide the target localization. This process is thus termed as Relevant Reasoning Segmentation (R<sup>2</sup>S), and it contains two steps as follows.

**Step 1: Reasoning Prior Learning.** While the model may encounter challenges in understanding intricate inter-object relationships, it can recognize objects relevant to the target. As shown in Fig. 2, despite the model’s limitation in accurately segmenting the chair beside the desk supporting a monitor, it demonstrates the ability to detect desks and chairs. Given this capability, we may instruct the model to initially segment approximate question-related objects, thus establishing the visual reasoning prior as the hint to help identify the final target.

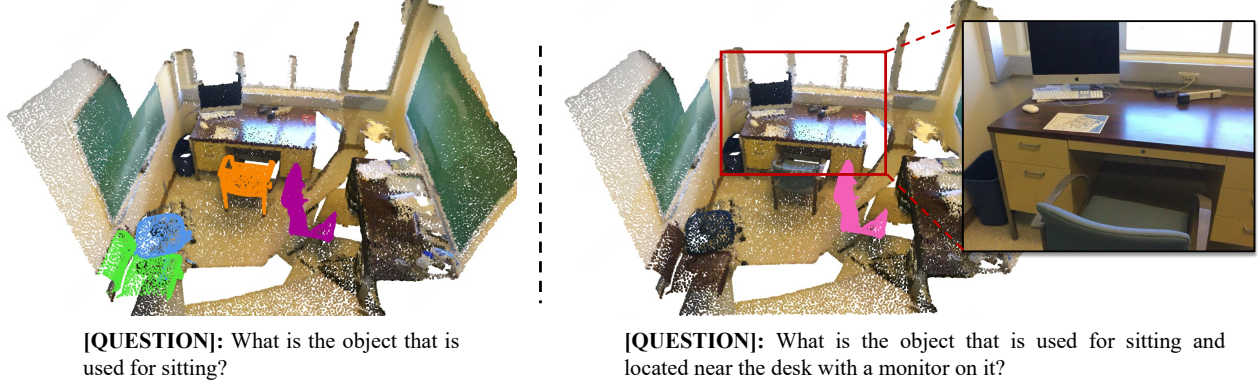


Figure 2. The image on the left depicts the LLM’s response to the question “What is the object that is used for sitting?” Conversely, the right side of the image illustrates the LLM’s response to the question “What is the object that is used for sitting and located *near the desk with a monitor on it*” It is noteworthy that the LLM provides an incorrect answer in the latter case. The accurate response should identify the chair within the red rectangle.

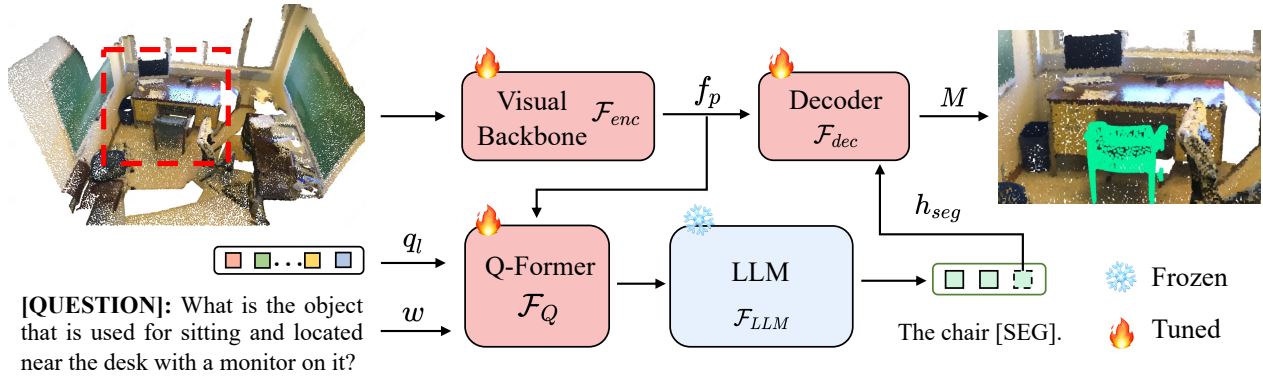


Figure 3. The baseline model consists of a visual backbone for point feature encoding, a Q-Former that connects visual-language representations, a LLM for instruction processing, and a mask decoder that converts [SEG] tokens into segmentation masks.

Following the baseline model’s process, we first use an instruction structured as: “Given the 3D scene, [QUESTION]. Please segment the question-related objects that may help answer the question.”<sup>1</sup> The corresponding instruction embedding  $w$  will be processed by Eq. (1) and Eq. (2) to obtain the text output  $y_{txt}$  from which we can obtain the [SEG] tokens representing these target-relevant objects. Subsequently, the segmentation head decodes the hidden features  $h_{seg}$  of [SEG] tokens into masks  $M_r$  for these target-relevant objects.

Next, we adopt mask-pooling to aggregate the superpoint features  $f_p$  with masks  $M_r$ , yielding the representations  $f_r$  for the target-relevant objects. The features  $f_r$  serve as the reasoning priors in the subsequent step. The above process can be formally expressed as:

$$M_r = \mathcal{F}_{dec}(f_p, h_{seg}), \quad (6)$$

<sup>1</sup>More templates are shown in the supplementary file

$$f_r = f_p \times M_r \quad (7)$$

**Step 2: Prior-guided Refinement.** In the absence of explicit instructions, the latent queries  $\hat{q}_l$  derived from Eq. (1) may exhibit a bias towards irrelevant areas, potentially impacting the reasoning process in Eq. (2). Besides, the mask-pooling operation in Eq. (7) may cause the loss of essential spatial details. Therefore, we propose the prior-guided refinement which commences by feeding the initial latent queries  $q_l$ , text outputs  $y_{txt}$  and target-relevant features  $f_r$  from step 1 into the Q-Former  $\mathcal{F}_Q$  to yield the refined query  $q'_l$  and target-relevant features  $f'_r$ .

To make use of the obtained reasoning priors, we employ a revised instruction like: “Given the 3D scene, the question is [QUESTION]. Please answer the question and output segmentation mask. The question-related objects are  $\{f_r^1, f_r^2, \dots, f_r^n\}$ , and you may need to pay

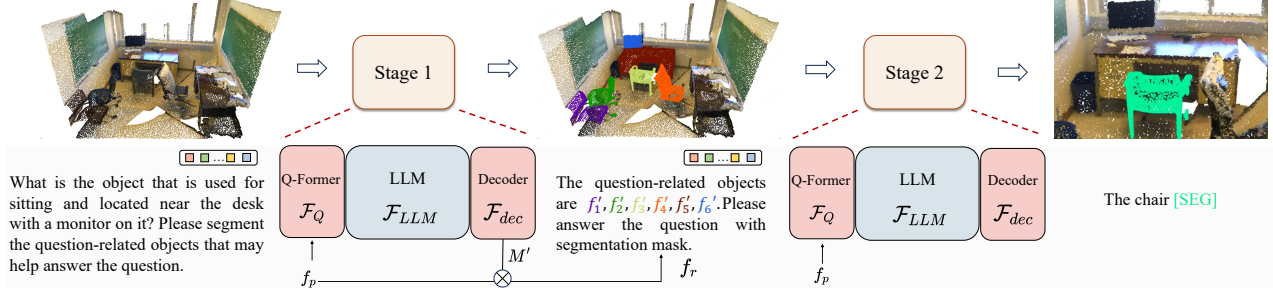


Figure 4. The proposed Relevant Reasoning Segmentation framework. Stage 1 segments question-related objects as priors ( $f'_1, \dots, f'_6$ ). Stage 2 refines hidden representations of instructions based on these priors, enabling the LLM to generate more accurate responses.

attention to them”<sup>2</sup> where the target-relevant features  $f_r$  of  $n$  potentially relevant objects have been inserted to form the new instruction whose text embedding is therefore denoted as  $w' \oplus f_r$ . To this end, the prior-guided refinement regarding the latent query and the target-relevant features can be formulated as:

$$q'_l, f'_r = \mathcal{F}_Q(q_l, w' \oplus f_r, f_p) \quad (8)$$

where  $w'$  and  $f_p$  are the text embeddings and super-point features, respectively. Unlike Eq. (3), during the prior-guided refinement,  $q_l$  is concatenated with the instruction embedding  $w' \oplus f_r$  to serve as the queries for both self-attention and cross-attention layers in the Q-Former  $\mathcal{F}_Q$ . Meanwhile,  $f_p$  continues to function as the key and value in the cross-attention layer. In Eq. (8), the enhanced latent query  $q'_l$  has been enriched with target-related clues from  $f_r$ . Simultaneously, utilizing the point-cloud features  $f_p$ , the target-relevant features  $f_r$  are refined with essential spatial intricacies to produce  $f'_r$ . Next, the refined query  $q'_l$  and target-relevant features  $f'_r$  are adopted for generating the new text output  $y'_{txt}$  with the LLM  $\mathcal{F}_{LLM}$ :

$$y'_{txt} = \mathcal{F}_{LLM}(q'_l, w' \oplus f'_r), \quad (9)$$

where the instruction embedding  $w' \oplus f_r$  originally used in Eq. (8) has been accordingly updated to  $w' \oplus f'_r$ . The hidden features  $h'_{seg}$  of the [SEG] tokens are extracted from the new text output  $y'_{txt}$  and processed by the decoder  $\mathcal{F}_{dec}$  to generate the refined final mask prediction  $M'$ :

$$M' = \mathcal{F}_{dec}(h'_{seg}, f_p) \quad (10)$$

### 3.3. 3D ReasonSeg

Analysis of existing datasets, as demonstrated in Fig. 5, reveals that spatial relations such as “in front of” often lack complexity and exhibit potential ambiguity. Using such datasets for training and evaluation may inadequately address the spatial reasoning requirements of 3D MLLMs. To

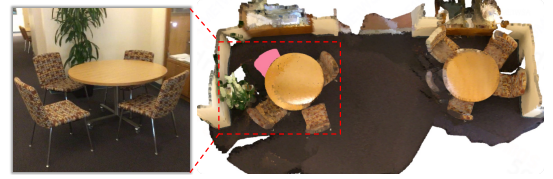


Figure 5. This illustrates a data sample from ScanRefer, where the target object is described as “A brown chair placed in front of a plant.” The spatial relationship in this description shows ambiguity, as there are multiple chairs in front of the plant.

facilitate enhancement and assessment of spatial reasoning capabilities in 3D MLLMs, we present 3D ReasonSeg, a dataset specifically designed for reasoning tasks in 3D point cloud environments. Empirical results in Tab. 2 indicate that models trained on 3D ReasonSeg achieve substantial performance improvements over baseline implementations.

Specifically, the proposed 3D ReasonSeg requires the model to identify the target object based on a question that does not explicitly mention it. The model needs to understand the object functions, visual attributes, and spatial relationships of the objects described in the query and reason to segment the target object. To implement this task, we use a template structured as: “**USER:** Given the 3D scene, please answer the question and output segmentation mask: [QUESTION]. **ASSISTANT:** [ANSWER]”.

We construct the 3D ReasonSeg dataset by integrating SceneVerse’s [22] detailed object descriptions with Llama 3.1 [15]. Based on objects’ 3D spatial information (positions and sizes) from point clouds and the object descriptions from SceneVerse, Llama 3.1 generates question-reasoning-answer pairs for reasoning tasks.

After collecting numerous question-reasoning-answer pairs, we apply rule-based filtering (e.g., calculating distances between objects and removing outliers) to eliminate instances with unclear or incorrect spatial relationships. The resulting 3D ReasonSeg dataset contains 29,151 high-quality data samples. Examples are shown in Fig. 6, with

<sup>2</sup>More templates are shown in the supplementary file.

details provided in the supplementary material.

We conduct a statistical analysis of ScanQA, ScanRefer, and 3D ReasonSeg datasets, examining their training (#Train) and validation (#Val) set sizes, average word counts per sample (Avg. Words), and average number of relevant objects (Avg. Objects). The detailed statistics are summarized in Tab. 1, showing that our proposed 3D ReasonSeg dataset contains more complex object relationships.

Dataset	#Train	#Val	Avg. Words	Avg. Objects
ScanQA	26,563	4,675	8.8	1.5
ScanRefer	36,665	9,508	17.8	1.8
3D ReasonSeg	25,185	3,966	19.6	<b>5.4</b>

Table 1. Comparative statistics across ScanQA, ScanRefer, and 3D ReasonSeg datasets.

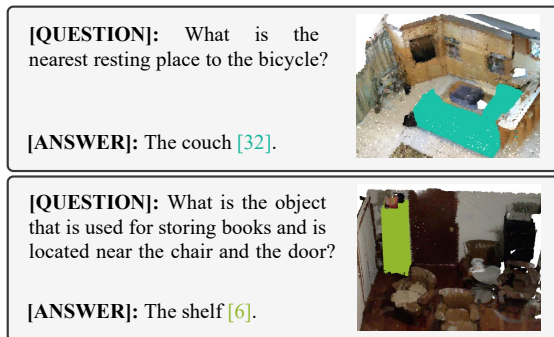


Figure 6. Visualization of 3D ReasonSeg samples, where instance ID colors correspond to their respective object colors in the image.

### 3.4. Model Training

**Training Datasets.** Following [6], our training data includes established 3D datasets such as ScanQA [2], ScanRefer [4], ScanNet200 [11], the ScanNet subset of 3D-LLM [18], and SceneVerse [22], along with our proposed 3D ReasonSeg dataset.

For Relevant Reasoning Segmentation outlined in Sec. 3.2, we extend the ScanQA, Scanrefer, and 3D ReasonSeg to incorporate target-relevant object identification. This process leverages scene object annotations and question-answer pairs from the original datasets, with Llama 3.1 [15] serving as the backbone for target-relevant object identification. Representative examples are presented in Fig. 7, with detailed prompts and implementation procedures in the supplementary material.

**Loss Function.** During training, the model is optimized using the cross-entropy loss  $\mathcal{L}_{txt}$  for text generation, along with the binary cross-entropy (BCE) and DICE losses ( $\mathcal{L}_{bce}$  and  $\mathcal{L}_{dice}$ ) for segmentation. Following [25], we assign equal weights of 1 to the BCE and DICE loss. Thus, the

overall training objective  $\mathcal{L}$  can be expressed as:

$$\mathcal{L} = \lambda_{txt}\mathcal{L}_{txt} + \mathcal{L}_{bce} + \mathcal{L}_{dice} \quad (11)$$

where  $\lambda_{txt}$  is the weight for text generation loss.

**Relevant Objects Augmentation.** Our relevant segmentation leverages mask predictions of relevant objects as priors to enhance latent query and text embedding. However, direct implementation leads to overfitting during training, as the ground truth relevant objects remain fixed during training but vary during inference, creating a train-test discrepancy. To address this issue, we implement random omission and addition of relevant objects during training, simulating diverse inference scenarios with incomplete priors.

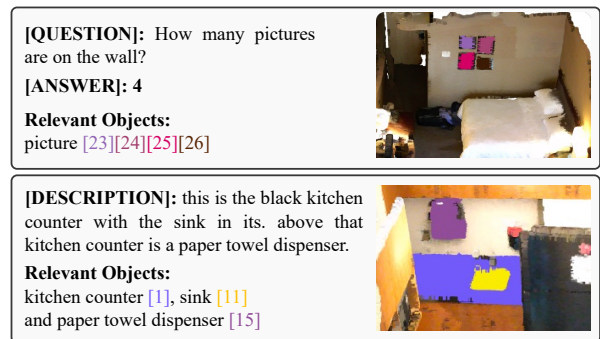


Figure 7. Examples of target-relevant data. The first row shows an instance from ScanQA, and the second row is related to ScanRefer. The visualizations of target-relevant objects are displayed on the right side of each row.

## 4. Experiments

### 4.1. Experimental Setting

**Implementation Details.** We adopt the encoder of a pre-trained Oneformer3D as visual backbone and the decoder of it as the mask decoder, and a pre-trained OPT 1.3B [57] as the language model. To preserve the learned knowledge of the pre-trained language model, we completely freeze the parameters of the language model while fully training the parameters of all other modules. Note that, we found it is necessary to also fine-tune the visual backbone. We adopt the AdamW [31] optimizer with a weight decay of 0.1 and a learning rate decaying from  $1e-4$  to  $1e-6$  with a cosine annealing scheduler. The text generation loss weight  $\lambda_{txt}$  is set to 0.5. The number of learnable queries in Q-Former is set to 32. We randomly sample 300k points from each 3D scene as the 3D input. All the experiments are conducted on eight Nvidia H20 GPUs.

**Benchmark and Metrics.** In this study, we assess our methods on ScanQA [2], ScanRefer [4], and our proposed 3D ReasonSeg. ScanQA is a dataset for the 3D question answering task, evaluating visual and spatial comprehension

Method	ScanRefer		ScanQA				3D ReasonSeg
	Acc@25	Acc@50	B-4 ↑	C ↑	M ↑	R ↑	gIoU
ScanRefer [4]	37.3	24.3	–	–	–	–	–
MVT [21]	40.8	33.3	–	–	–	–	–
3DVG-Trans [59]	45.9	34.5	–	–	–	–	–
ViL3DRel [5]	47.9	37.7	–	–	–	–	–
M3DRef-CLIP [58]	51.9	44.7	–	–	–	–	–
ScanQA [2]	–	–	10.1	64.9	13.1	33.3	–
3D-VisTA [62]	50.6	45.8	13.1	72.9	–	–	–
LLM-Grounder [51]	17.1	5.3	–	–	–	–	–
3D-LLM [18]	30.3	–	12.0	69.4	14.5	35.7	–
Chat-3D [48]	–	–	6.4	53.2	11.9	28.5	–
Chat-3D v2 [19]	35.9	30.4	7.3	77.1	16.1	<b>40.1</b>	–
LL3DA [6]	–	–	13.5	76.8	15.9	37.3	–
ScanReason [60]	53.1	41.1	–	–	–	–	–
Grounded 3D-LLM [9]	47.9	44.1	13.4	72.7	–	–	25.6
baseline	54.6	38.7	12.8	70.5	13.8	34.6	–
+ 3D ReasonSeg	58.9	43.6	13.3	75.2	15.5	36.7	29.2
+ R <sup>2</sup> S	<b>59.5</b>	<b>48.7</b>	<b>13.9</b>	<b>77.3</b>	<b>16.4</b>	38.1	<b>33.1</b>

Table 2. Results among our methods and previous related works. Entries in gray denote models specialized for specific datasets.

of 3D environments. The evaluation metrics of ScanQA include BLEU-4, CIDEr, METEOR, and Rouge-L. ScanRefer evaluates the capability to localize 3D object using a natural language description. Prediction accuracy is measured by the percentage of predictions with Intersection over Union (IoU) above 0.25 and 0.5 compared to ground truth masks. For 3D ReasonSeg, the model is required to focus on object attributes and relationships to reason, answering questions and localizing target objects. Following [26], the general Intersection over Union (gIoU) metric is used, defined as the average of all per-scene Intersection-over-Unions (IoUs). Detailed formulations of these tasks can be found in the supplementary material.

## 4.2. Main Results

We evaluate our model’s effectiveness through comprehensive comparisons with state-of-the-art (SOTA) methods, encompassing both task-specific specialist models and multi-task generalist models. For a fair comparison, we finetune Grounded 3D-LLM [9], the previous SOTA model on ScanRefer, on our proposed 3D ReasonSeg dataset and assess its performance on the 3D ReasonSeg benchmark.

As shown in Tab. 2, our baseline model is comparable to existing approaches on both ScanRefer and ScanQA. While our baseline model demonstrates robust performance, the incorporation of 3D ReasonSeg and R<sup>2</sup>S yields consistent substantial improvements across all metrics, validating the effectiveness of our approach. Notably, R<sup>2</sup>S significantly enhances the Acc@50 metric on ScanRefer and the gIoU

metric on 3D ReasonSeg, tasks that require robust spatial reasoning, aligning with our expectations.

Method	ScanRefer		ScanQA				3D ReasonSeg
	Acc@25	Acc@50	B-4 ↑	C ↑	M ↑	R ↑	gIoU
wo PR	58.2	41.3	7.7	66.1	13.4	33.2	27.5
text-based	58.4	43.5	13.7	75.5	15.6	36.9	29.8
R <sup>2</sup> S	<b>59.5</b>	<b>48.7</b>	<b>13.9</b>	<b>77.3</b>	<b>16.4</b>	<b>38.1</b>	<b>33.1</b>

Table 3. Ablation study on the Prior-guided Refinement.

number of latent queries	ScanRefer		ScanQA				3D ReasonSeg
	Acc@25	Acc@50	B-4 ↑	C ↑	M ↑	R ↑	gIoU
16	57.2	40.5	14.0	75.3	15.2	36.8	28.9
32	<b>58.9</b>	<b>43.6</b>	13.3	<b>75.2</b>	<b>15.5</b>	<b>36.7</b>	<b>29.2</b>
48	58.7	41.6	<b>14.5</b>	74.3	15.1	36.1	28.4

Table 4. Ablation study on the number of latent queries. The results are based on our base method.

$\lambda_{txt}$	ScanRefer		ScanQA				3D ReasonSeg
	Acc@25	Acc@50	B-4 ↑	C ↑	M ↑	R ↑	gIoU
0.1	61.3	43.9	12.3	68.2	14.3	34.0	28.9
0.5	<b>58.9</b>	<b>43.6</b>	<b>13.3</b>	<b>75.2</b>	<b>15.5</b>	<b>36.7</b>	<b>29.2</b>
1.0	58.7	41.4	13.2	72.6	15.2	35.6	28.6

Table 5. Ablation study on the loss weight configurations, where  $\lambda_{txt}$  means the weight of  $\mathcal{L}_{txt}$ .

**Effectiveness of Prior-guided Refinement.** To verify the necessity of Prior-guided Refinement (PR), we investigate the approach without PR (wo PR) and directly representing target-relevant objects as textual information (text-based). The results are shown in Tab. 3.



Figure 8. Visual qualitative results on ScanQA and 3D ReasonSeg.

When Prior-guided Refinement is removed, the model simultaneously predict relevant objects and process instructions. Results indicate that the approach without Prior-guided Refinement not only fails to improve performance but potentially degrades it. This degradation likely stems from the increased computational complexity of concurrent object prediction and instruction processing without supplementary contextual information.

The text-based method represents an ablation variant of R<sup>2</sup>S where segmentation information is omitted, providing only text prompts such as “The question-related objects are chairs, and you may need to pay attention to them”. Although text-based approach demonstrates modest improvements, our method consistently achieves superior results. This performance advantage can be attributed to our approach’s ability to extract precise instance-level visual features through segmentation masks. In contrast, text-based method fails to capture spatial information and demonstrates inherent limitations in differentiating multiple instances of identical categories within a scene (*e.g.*, multiple chairs).

**The Number of Latent Queries.** We investigate the number of Q-Former latent queries. As demonstrated in Tab. 4, experiments with 16, 32, and 48 latent queries reveal that 32 queries yield optimal performance.

**Loss Weight.** We conduct an ablation study on the text loss weight  $\lambda_{txt}$  using values of 0.1, 0.5, and 1.0. Our experi-

**USER:** What object is used for drying the body and is located on the towel rack near the bathtub? Please answer the question with segmentation mask.

**ASSISTANT:** the towel [SEG] ✗



**USER:** What object is used for drying the body and is located on the towel rack near the bathtub? Please answer the question with segmentation mask. The question-related objects are [SEG] [SEG][SEG][SEG], and you may need to pay attention to them.

**ASSISTANT:** the towel [SEG] ✓



ments demonstrate that setting  $\lambda_{txt}$  to 1.0 achieves optimal balance in performance, as evidenced in Tab. 5.

### 4.3. Qualitative Results

As illustrated in Fig. 8, we present a comparison between the baseline and R<sup>2</sup>S. The left portion of the figure compares baseline predictions (upper row) with R<sup>2</sup>S predictions (lower row) for ScanQA. The lower row shows segmentation results for target-relevant objects. Similarly, the right portion compares baseline and R<sup>2</sup>S predictions for 3D ReasonSeg. Additional qualitative results are provided in the supplementary material.

## 5. Limitation

Due to the use of large language models for data generation instead of human annotation, some noise remains in our dataset even after data cleaning procedures, potentially impacting model performance. We will further optimize our dataset in future work.

## 6. Conclusions

In this paper, we introduce the Relevant Reasoning Segmentation framework, a reasoning-based segmentation framework that enhances spatial reasoning by emulating human reasoning processes through Reasoning Prior Learning and Prior-guided Refinement. Furthermore, we propose 3D ReasonSeg, a reasoning-based segmentation

dataset designed to enhance and comprehensively assess the spatial reasoning capabilities in 3D MLLMs. We hope our work provides new insights and directions for exploring the spatial reasoning capabilities in 3D MLLMs.

## References

- [1] Jean-Baptiste Alayrac, Jeff Donahue, Pauline Luc, Antoine Miech, Iain Barr, Yana Hasson, Karel Lenc, Arthur Mensch, Katherine Millican, Malcolm Reynolds, et al. Flamingo: a visual language model for few-shot learning. Advances in neural information processing systems, 35:23716–23736, 2022. 1
- [2] Daichi Azuma, Taiki Miyanishi, Shuhei Kurita, and Motoaki Kawanabe. Scanqa: 3d question answering for spatial scene understanding. In proceedings of the IEEE/CVF conference on computer vision and pattern recognition, pages 19129–19139, 2022. 2, 6, 7, 12
- [3] Yingjie Cai, Xuesong Chen, Chao Zhang, Kwan-Yee Lin, Xiaogang Wang, and Hongsheng Li. Semantic scene completion via integrating instances and scene in-the-loop. In Proceedings of the IEEE/CVF Conference on Computer Vision and Pattern Recognition, pages 324–333, 2021. 2
- [4] Dave Zhenyu Chen, Angel X Chang, and Matthias Nießner. Scanrefer: 3d object localization in rgb-d scans using natural language. In European conference on computer vision, pages 202–221. Springer, 2020. 2, 6, 7, 12
- [5] Shizhe Chen, Pierre-Louis Guhur, Makarand Tapaswi, Cordelia Schmid, and Ivan Laptev. Language conditioned spatial relation reasoning for 3d object grounding. Advances in neural information processing systems, 35:20522–20535, 2022. 7
- [6] Sijin Chen, Xin Chen, Chi Zhang, Mingsheng Li, Gang Yu, Hao Fei, Hongyuan Zhu, Jiayuan Fan, and Tao Chen. Ll3da: Visual interactive instruction tuning for omni-3d understanding reasoning and planning. In Proceedings of the IEEE/CVF Conference on Computer Vision and Pattern Recognition, pages 26428–26438, 2024. 1, 2, 3, 6, 7
- [7] Xuesong Chen, Shaoshuai Shi, Benjin Zhu, Ka Chun Cheung, Hang Xu, and Hongsheng Li. Mppnet: Multi-frame feature intertwining with proxy points for 3d temporal object detection. In European Conference on Computer Vision, pages 680–697. Springer, 2022. 2
- [8] Xuesong Chen, Shaoshuai Shi, Chao Zhang, Benjin Zhu, Qiang Wang, Ka Chun Cheung, Simon See, and Hongsheng Li. Trajectoryformer: 3d object tracking transformer with predictive trajectory hypotheses. In Proceedings of the IEEE/CVF International Conference on Computer Vision, pages 18527–18536, 2023. 2
- [9] Yilun Chen, Shuai Yang, Haifeng Huang, Tai Wang, Ruiyuan Lyu, Runsen Xu, Dahua Lin, and Jiangmiao Pang. Grounded 3d-llm with referent tokens. arXiv preprint arXiv:2405.10370, 2024. 2, 7
- [10] Jiequan Cui, Shu Liu, Zhuotao Tian, Zhisheng Zhong, and Jiaya Jia. Reslt: Residual learning for long-tailed recognition. IEEE transactions on pattern analysis and machine intelligence, 45(3):3695–3706, 2022. 12
- [11] Angela Dai, Angel X Chang, Manolis Savva, Maciej Halber, Thomas Funkhouser, and Matthias Nießner. Scannet: Richly-annotated 3d reconstructions of indoor scenes. In Proceedings of the IEEE conference on computer vision and pattern recognition, pages 5828–5839, 2017. 6
- [12] Anurag Das, Xinting Hu, Li Jiang, and Bernt Schiele. Mta-clip: Language-guided semantic segmentation with mask-text alignment. arXiv preprint arXiv:2407.21654, 2024. 2
- [13] Jacob Devlin. Bert: Pre-training of deep bidirectional transformers for language understanding. arXiv preprint arXiv:1810.04805, 2018. 12, 14
- [14] Runyu Ding, Jihan Yang, Chuhui Xue, Wenqing Zhang, Song Bai, and Xiaojuan Qi. Pla: Language-driven open-vocabulary 3d scene understanding. In Proceedings of the IEEE/CVF conference on computer vision and pattern recognition, pages 7010–7019, 2023. 2
- [15] Abhimanyu Dubey, Abhinav Jauhri, Abhinav Pandey, Abhishek Kadian, Ahmad Al-Dahle, Aiesha Letman, and Akhil Mathur et.al. The llama 3 herd of models, 2024. 5, 6, 12
- [16] Ziyu Guo, Renrui Zhang, Xiangyang Zhu, Yiwen Tang, Xi-anzheng Ma, Jiaming Han, Kexin Chen, Peng Gao, Xi-anzhi Li, Hongsheng Li, et al. Point-bind & point-llm: Aligning point cloud with multi-modality for 3d understanding, generation, and instruction following. arXiv preprint arXiv:2309.00615, 2023. 2
- [17] Jiaming Han, Renrui Zhang, Wenqi Shao, Peng Gao, Peng Xu, Han Xiao, Kaipeng Zhang, Chris Liu, Song Wen, Ziyu Guo, et al. Imagebind-llm: Multi-modality instruction tuning. arXiv preprint arXiv:2309.03905, 2023. 2
- [18] Yining Hong, Haoyu Zhen, Peihao Chen, Shuhong Zheng, Yilun Du, Zhenfang Chen, and Chuang Gan. 3d-llm: Injecting the 3d world into large language models. Advances in Neural Information Processing Systems, 36:20482–20494, 2023. 1, 2, 3, 6, 7
- [19] Haifeng Huang, Zehan Wang, Rongjie Huang, Luping Liu, Xize Cheng, Yang Zhao, Tao Jin, and Zhou Zhao. Chat-3d v2: Bridging 3d scene and large language models with object identifiers. arXiv preprint arXiv:2312.08168, 2023. 1, 2, 3, 7
- [20] Jiangyong Huang, Silong Yong, Xiaojian Ma, Xiongkun Linghu, Puhao Li, Yan Wang, Qing Li, Song-Chun Zhu, Baoxiong Jia, and Siyuan Huang. An embodied generalist agent in 3d world. arXiv preprint arXiv:2311.12871, 2023. 2
- [21] Shijia Huang, Yilun Chen, Jiaya Jia, and Liwei Wang. Multi-view transformer for 3d visual grounding. In Proceedings of the IEEE/CVF Conference on Computer Vision and Pattern Recognition, pages 15524–15533, 2022. 2, 7
- [22] Baoxiong Jia, Yixin Chen, Huangyue Yu, Yan Wang, Xuesong Niu, Tengyu Liu, Qing Li, and Siyuan Huang. Sceneverse: Scaling 3d vision-language learning for grounded scene understanding. arXiv preprint arXiv:2401.09340, 2024. 5, 6
- [23] Li Jiang, Shaoshuai Shi, Zhuotao Tian, Xin Lai, Shu Liu, Chi-Wing Fu, and Jiaya Jia. Guided point contrastive learning for semi-supervised point cloud semantic segmentation.

- In Proceedings of the IEEE/CVF international conference on computer vision, pages 6423–6432, 2021. [12](#)
- [24] Alexander Kirillov, Eric Mintun, Nikhila Ravi, Hanzi Mao, Chloe Rolland, Laura Gustafson, Tete Xiao, Spencer Whitehead, Alexander C. Berg, Wan-Yen Lo, Piotr Dollár, and Ross Girshick. Segment anything. arXiv preprint arXiv:2304.02643, 2023. [3](#)
- [25] Maxim Kolodiaznyy, Anna Vorontsova, Anton Konushin, and Danila Rukhovich. Oneformer3d: One transformer for unified point cloud segmentation. In Proceedings of the IEEE/CVF Conference on Computer Vision and Pattern Recognition, pages 20943–20953, 2024. [2](#), [6](#), [12](#), [14](#)
- [26] Xin Lai, Zhuotao Tian, Yukang Chen, Yanwei Li, Yuhui Yuan, Shu Liu, and Jiaya Jia. Lisa: Reasoning segmentation via large language model. In Proceedings of the IEEE/CVF Conference on Computer Vision and Pattern Recognition, pages 9579–9589, 2024. [3](#), [7](#)
- [27] Xin Lai, Zhuotao Tian, Yukang Chen, Senqiao Yang, Xiangru Peng, and Jiaya Jia. Step-dpo: Step-wise preference optimization for long-chain reasoning of llms. arXiv preprint arXiv:2406.18629, 2024. [12](#)
- [28] Loic Landrieu and Martin Simonovsky. Large-scale point cloud semantic segmentation with superpoint graphs. In Proceedings of the IEEE conference on computer vision and pattern recognition, pages 4558–4567, 2018. [3](#)
- [29] Junnan Li, Dongxu Li, Silvio Savarese, and Steven Hoi. Blip-2: Bootstrapping language-image pre-training with frozen image encoders and large language models. In International conference on machine learning, pages 19730–19742. PMLR, 2023. [1](#), [3](#), [12](#), [14](#)
- [30] Dingning Liu, Xiaoshui Huang, Yuenan Hou, Zhihui Wang, Zhenfei Yin, Yongshun Gong, Peng Gao, and Wanli Ouyang. Uni3d-llm: Unifying point cloud perception, generation and editing with large language models. arXiv preprint arXiv:2402.03327, 2024. [2](#)
- [31] I Loshchilov. Decoupled weight decay regularization. arXiv preprint arXiv:1711.05101, 2017. [6](#)
- [32] Xiaojian Ma, Silong Yong, Zilong Zheng, Qing Li, Yitao Liang, Song-Chun Zhu, and Siyuan Huang. Sqa3d: Situated question answering in 3d scenes. arXiv preprint arXiv:2210.07474, 2022. [2](#)
- [33] Ishan Misra, Rohit Girdhar, and Armand Joulin. An end-to-end transformer model for 3d object detection. In Proceedings of the IEEE/CVF international conference on computer vision, pages 2906–2917, 2021. [2](#)
- [34] Zhenhua Ning, Zhuotao Tian, Guangming Lu, and Wenjie Pei. Boosting few-shot 3d point cloud segmentation via query-guided enhancement. In Proceedings of the 31st ACM international conference on multimedia, pages 1895–1904, 2023. [12](#)
- [35] Bohao Peng, Zhuotao Tian, Xiaoyang Wu, Chengyang Wang, Shu Liu, Jingyong Su, and Jiaya Jia. Hierarchical dense correlation distillation for few-shot segmentation. In Proceedings of the IEEE/CVF Conference on Computer Vision and Pattern Recognition, pages 23641–23651, 2023. [12](#)
- [36] Bohao Peng, Zhuotao Tian, Shu Liu, Mingchang Yang, and Jiaya Jia. Scalable language model with generalized continual learning. arXiv preprint arXiv:2404.07470, 2024. [12](#)
- [37] Bohao Peng, Xiaoyang Wu, Li Jiang, Yukang Chen, Hengshuang Zhao, Zhuotao Tian, and Jiaya Jia. Oa-cnns: Omni-adaptive sparse cnns for 3d semantic segmentation. In Proceedings of the IEEE/CVF Conference on Computer Vision and Pattern Recognition, pages 21305–21315, 2024. [12](#)
- [38] Songyou Peng, Kyle Genova, Chiyu Jiang, Andrea Tagliasacchi, Marc Pollefeys, Thomas Funkhouser, et al. Openscene: 3d scene understanding with open vocabularies. In Proceedings of the IEEE/CVF conference on computer vision and pattern recognition, pages 815–824, 2023. [2](#)
- [39] Tong Shao, Zhuotao Tian, Hang Zhao, and Jingyong Su. Explore the potential of clip for training-free open vocabulary semantic segmentation. In European Conference on Computer Vision, pages 139–156. Springer, 2024. [12](#)
- [40] Shaoshuai Shi, Xiaogang Wang, and Hongsheng Li. Pointcnn: 3d object proposal generation and detection from point cloud. In Proceedings of the IEEE/CVF conference on computer vision and pattern recognition, pages 770–779, 2019. [2](#)
- [41] Ayça Takmaz, Elisabetta Fedele, Robert W Sumner, Marc Pollefeys, Federico Tombari, and Francis Engelmann. Openmask3d: Open-vocabulary 3d instance segmentation. arXiv preprint arXiv:2306.13631, 2023. [2](#)
- [42] Longxiang Tang, Zhuotao Tian, Kai Li, Chunming He, Hantao Zhou, Hengshuang Zhao, Xiu Li, and Jiaya Jia. Mind the interference: Retaining pre-trained knowledge in parameter efficient continual learning of vision-language models. In European Conference on Computer Vision, pages 346–365. Springer, 2024. [12](#)
- [43] Zhuotao Tian, Michelle Shu, Pengyuan Lyu, Ruiyu Li, Chao Zhou, Xiaoyong Shen, and Jiaya Jia. Learning shape-aware embedding for scene text detection. In Proceedings of the IEEE/CVF conference on computer vision and pattern recognition, pages 4234–4243, 2019. [12](#)
- [44] Zhuotao Tian, Hengshuang Zhao, Michelle Shu, Zhicheng Yang, Ruiyu Li, and Jiaya Jia. Prior guided feature enrichment network for few-shot segmentation. IEEE transactions on pattern analysis and machine intelligence, 44(2):1050–1065, 2020. [12](#)
- [45] Zhuotao Tian, Pengguang Chen, Xin Lai, Li Jiang, Shu Liu, Hengshuang Zhao, Bei Yu, Ming-Chang Yang, and Jiaya Jia. Adaptive perspective distillation for semantic segmentation. IEEE Transactions on Pattern Analysis and Machine Intelligence, 45(2):1372–1387, 2022. [12](#)
- [46] Zhuotao Tian, Xin Lai, Li Jiang, Shu Liu, Michelle Shu, Hengshuang Zhao, and Jiaya Jia. Generalized few-shot semantic segmentation. In Proceedings of the IEEE/CVF Conference on Computer Vision and Pattern Recognition, pages 11563–11572, 2022. [12](#)
- [47] Zhuotao Tian, Jiequan Cui, Li Jiang, Xiaojuan Qi, Xin Lai, Yixin Chen, Shu Liu, and Jiaya Jia. Learning context-aware classifier for semantic segmentation. In Proceedings of the AAAI Conference on Artificial Intelligence, pages 2438–2446, 2023. [12](#)

- [48] Zehan Wang, Haifeng Huang, Yang Zhao, Ziang Zhang, and Zhou Zhao. Chat-3d: Data-efficiently tuning large language model for universal dialogue of 3d scenes. [arXiv preprint arXiv:2308.08769](#), 2023. 1, 2, 7
- [49] Chenfei Wu, Shengming Yin, Weizhen Qi, Xiaodong Wang, Zecheng Tang, and Nan Duan. Visual chatgpt: Talking, drawing and editing with visual foundation models. [arXiv preprint arXiv:2303.04671](#), 2023. 1
- [50] Runsen Xu, Xiaolong Wang, Tai Wang, Yilun Chen, Jiangmiao Pang, and Dahua Lin. Pointllm: Empowering large language models to understand point clouds. [arXiv preprint arXiv:2308.16911](#), 2023. 1, 2
- [51] Jianing Yang, Xuweiyi Chen, Shengyi Qian, Nikhil Madaan, Madhavan Iyengar, David F Fouhey, and Joyce Chai. Llm-grounder: Open-vocabulary 3d visual grounding with large language model as an agent. In [2024 IEEE International Conference on Robotics and Automation \(ICRA\)](#), pages 7694–7701. IEEE, 2024. 7
- [52] Senqiao Yang, Tianyuan Qu, Xin Lai, Zhuotao Tian, Bohao Peng, Shu Liu, and Jiaya Jia. Lisa++: An improved baseline for reasoning segmentation with large language model. [arXiv preprint arXiv:2312.17240](#), 2023. 12
- [53] Senqiao Yang, Zhuotao Tian, Li Jiang, and Jiaya Jia. Unified language-driven zero-shot domain adaptation. In [Proceedings of the IEEE/CVF Conference on Computer Vision and Pattern Recognition](#), pages 23407–23415, 2024.
- [54] Senqiao Yang, Yukang Chen, Zhuotao Tian, Chengyao Wang, Jingyao Li, Bei Yu, and Jiaya Jia. Visionzip: Longer is better but not necessary in vision language models. In [Proceedings of the Computer Vision and Pattern Recognition Conference](#), pages 19792–19802, 2025. 12
- [55] Zhengyuan Yang, Linjie Li, Jianfeng Wang, Kevin Lin, Ehsan Azarnasab, Faisal Ahmed, Zicheng Liu, Ce Liu, Michael Zeng, and Lijuan Wang. Mm-react: Prompting chatgpt for multimodal reasoning and action. [arXiv preprint arXiv:2303.11381](#), 2023. 1
- [56] Qinghao Ye, Haiyang Xu, Guohai Xu, Jiabo Ye, Ming Yan, Yiyang Zhou, Junyang Wang, Anwen Hu, Pengcheng Shi, Yaya Shi, et al. mplug-owl: Modularization empowers large language models with multimodality. [arXiv preprint arXiv:2304.14178](#), 2023. 1
- [57] Susan Zhang, Stephen Roller, Naman Goyal, Mikel Artetxe, Moya Chen, Shuohui Chen, Christopher Dewan, Mona Diab, Xian Li, Xi Victoria Lin, et al. Opt: Open pre-trained transformer language models. [arXiv preprint arXiv:2205.01068](#), 2022. 6
- [58] Yiming Zhang, ZeMing Gong, and Angel X Chang. Multi3drefer: Grounding text description to multiple 3d objects. In [Proceedings of the IEEE/CVF International Conference on Computer Vision](#), pages 15225–15236, 2023. 2, 7
- [59] Lichen Zhao, Daigang Cai, Lu Sheng, and Dong Xu. 3dvg-transformer: Relation modeling for visual grounding on point clouds. In [Proceedings of the IEEE/CVF International Conference on Computer Vision](#), pages 2928–2937, 2021. 7
- [60] Chenming Zhu, Tai Wang, Wenwei Zhang, Kai Chen, and Xihui Liu. Empowering 3d visual grounding with reasoning capabilities. [arXiv preprint arXiv:2407.01525](#), 2024. 2, 7
- [61] Deyao Zhu, Jun Chen, Xiaoqian Shen, Xiang Li, and Mohamed Elhoseiny. Minigt-4: Enhancing vision-language understanding with advanced large language models. [arXiv preprint arXiv:2304.10592](#), 2023. 1
- [62] Ziyu Zhu, Xiaojian Ma, Yixin Chen, Zhidong Deng, Siyuan Huang, and Qing Li. 3d-vista: Pre-trained transformer for 3d vision and text alignment. In [Proceedings of the IEEE/CVF International Conference on Computer Vision](#), pages 2911–2921, 2023. 7

## A. Data construction details.

**Data construction prompts.** The prompt used for data generation is illustrated in Fig. 9. We instruct LLama3.1 [15] to create question-reasoning-answer pairs and specify the target-relevant objects in the intermediate reasoning steps. The prompt used to construct target-relevant objects for ScanQA and ScanRefer is depicted in Fig. 10. We instruct LLama3.1 based on the objects’ spatial information and annotations from ScanQA and ScanRefer.

**Rule-based filtering.** In the context of rule-based filtering, we conducted a manual examination of the generated data and formulated filtering strategies. Firstly, we removed data containing phrases such as “in the right of” to mitigate potential ambiguity in 3D space. Secondly, for data involving spatial relationships like “near”, we calculated the distances between the objects and filtered out data with distances surpassing a predefined threshold. Thirdly, in instances of superlative relationships like “largest” or “nearest”, we evaluated object center distances or sizes to validate their adherence to the criteria. Additionally, we excluded data that strayed from the specified prompt structure and identified and eliminated objects created by LLama3.1 based on point cloud instance labels. Furthermore, we pruned data exceeding a designated threshold of related objects and eliminated instances where each reasoning step yielded the same related objects to avoid redundancy. Lastly, we discarded data where reasoning conditions overlapped with reasoning results during inference and where the final step of reasoning conflicted with the answer to the question.

## B. Task formulation details

We introduce each instruction with the “**USER:**” and format all tasks as auto-regressive generation sequences under the “**ASSISTANT:**”.

**3D Question Answering** tasks the model with responding to questions based on a 3D scene. We utilize a structured format such as: “**USER:** Given the 3D scene, please answer the question: [QUESTION]. **ASSISTANT:** [ANSWER]”, where [QUESTION] and [ANSWER] are sourced from the ScanQA dataset.

**Scene Description** requires the model to describe the entire scene using natural language. We adopt a format like: “**USER:** Describe this scene. **ASSISTANT:** [DESCRIPTION]”, where [DESCRIPTION] is derived from 3D-LLM.

**3D Instance Segmentation** task involves segmenting object categories within a scene. Our template is: “**USER:** Please segment the category in this scene. **ASSISTANT:** Sure, the segment results are [SEG]...[SEG]”, where the [CATEGORY] is from ScanNet200 and each [SEG] corresponds to an individual object.

**3D Referring Segmentation** requires the model to

segment a target object based on a brief description. Our template is: “**USER:** Please segment this object: [DESCRIPTION]. **ASSISTANT:** Sure, the segment result is [SEG]”, where the [DESCRIPTION] is from ScanRefer and the [SEG] represents the segmentation mask of the target object.

**3D Reasoning Segmentation** necessitates understanding the visual attributes, functions, and relationships of objects to find the target. Our template is: “**USER:** Given the 3D scene, please answer the question with segmentation mask: [QUESTION]. **ASSISTANT:** [ANSWER]”, where [QUESTION] and [ANSWER] are sourced from the 3D ReasonSeg dataset.

**Relevant Reasoning Segmentation Templates.** The details of Relevant Reasoning Segmentation are outlined in the main text, and additional examples for R<sup>2</sup>S are shown in Fig. 11, covering question answering, reasoning segmentation, and referring.

Method	ScanQA	ScanRefer	3D ReasonSeg
base	0.15s	0.23s	0.29s
+ R <sup>2</sup> S	0.46s	0.62s	0.67s

Table 6. The efficiency of our proposed methods in ScanQA, ScanRefer and 3D ReasonSeg.

## C. Efficiency of Method.

As shown in Tab. 6, we have evaluated the inference time of our proposed methods on ScanQA [2], ScanRefer [4], and 3D ReasonSeg, utilizing a single H20 GPU.

## D. Additional Qualitative Results

Additional visual qualitative results of 3D ReasonSeg are shown in Fig. 12. Each row displays the user instruction, prediction, target-relevant objects, and ground truth. Further visual qualitative results of dialogue and embodied planning are depicted in Fig. 13.

## E. Additional Implementation Details

Recent advances in deep learning [23, 35, 37, 43, 44, 47], computer vision [10, 25, 34, 45, 46], and large language models [13, 27, 29, 36, 39, 42, 52–54] have significantly advanced the development of perception systems, inspiring our model design.

**Point Cloud Encoder.** We employ the UNet style SparseConv from OneFormer3D [25], pre-trained on ScanNet. The feature dimension in the Encoder rises from 32 to 160 and then decreases back to 32. The voxel size of the SparseConv is 0.02m. All the parameters of the Encoder are trainable during training.

Generate reasoning-based segmentation data from object annotations in a 3D scene. Each object annotation is structured as follows: {instance\_id: <id>, category: <category>, center: [<x>, <y>, <z>], sizes: [<length>, <width>, <height>], captions: [<captions>]}. Key points: 1. All measurements (coordinates and sizes) are in meters. 2. Objects with the same <ins\_id> are considered identical.

Task requirements:

1. Generate challenging object-centric questions using the annotations:
  - a. Focus on detecting and distinguishing objects. The answer should specify one or more objects.
  - b. Include at least two of the objects' uses, appearance, positions, and sizes.
  - c. Require logical reasoning to answer.
  - d. Ensure questions are specific with one clear answer.
  - e. Ensure object descriptions distinctly identify them from similar items.
2. Provide step-by-step reasoning for each question follow these steps:
  1. Analyze the properties and spatial relationship of objects in the scene.
  2. Analyze the question and identify question-related objects.
  3. Construct a logical step-by-step reasoning based on your analysis to answer the question.
  4. Present the reasoning steps clearly.
  5. Use [<ins\_id>] to refer objects in reasoning steps. For multiple objects of the same category, use [<ins\_id>][<ins\_id>][<ins\_id>], etc.
3. Answer the question accurately.
4. Only use objects from the annotations.
5. Output format: 'question;reasoning;answer'. Don't output anything else.

Now generate for following annotations:

Figure 9. The prompt for yielding 3D ReasonSeg.

Generate step-by-step reasoning for question-answer pairs based on 3D scene object annotations. Each question-answer pair follows this structure: {question\_id: <question\_id>, question: <question>, answer: <answer>}. Object annotations are structured as: {instance\_id: <instance\_id>, category: <category>, center: [<x>, <y>, <z>], sizes: [<length>, <width>, <height>], captions: [<captions>]}. Key points: 1. All measurements (coordinates and sizes) are in meters. 2. Objects with the same <ins\_id> are considered identical.

Task requirements:

1. Process each question-answer pair, follow these steps:
  - a. Analyze the properties and spatial relationship of objects in the scene.
  - b. Analyze the question and identify question-related objects.
  - c. Construct a logical step-by-step reasoning based on your analysis to answer the question.
  - d. Present the reasoning steps clearly.
  - e. Use [<instance\_id>] to refer objects in reasoning steps.
  - f. Avoid mention the annotations.
2. Output format: '<question\_id>;reasoning'. Don't output anything else.

Now generate for following annotations:

---

List description-related objects in description of 3D scene object annotations. Object annotations are structured as: {annotation\_id: <annotation\_id>, instance\_id: <instance\_id>, category: <category>, description: <description>}. Key points: 1. All measurements (coordinates and sizes) are in meters. 2. Objects with the same <ins\_id> are considered identical.

Task requirements:

1. Analyze the properties and spatial relationship of objects in the scene based on the annotations.
2. Process each annotation, follow these steps:
  - a. Analyze the description and identify description-related objects.
  - b. Use [<instance\_id>] to refer description-related objects.
3. Output format: '<annotation\_id>;<description-related\_objects>'. Don't output any other things.

Now generate for following annotations:

Figure 10. The prompt for generating target-relevant objects for ScanQA and ScanRefer.

Task Name	Instruction Template
3D Reasoning Segmentation	<b>USER:</b> Given the 3D scene, please answer the question with segmentation mask: [QUESTION]. <b>ASSISTANT:</b> [ANSWER] <b>USER:</b> Please answer the question and output corresponding segmentation mask: [QUESTION]. <b>ASSISTANT:</b> [ANSWER]
3D Question Answering	<b>USER:</b> Given the 3D scene, please answer the question: [QUESTION]. <b>ASSISTANT:</b> [ANSWER] <b>USER:</b> Answer the question based on the 3D scene: [QUESTION]. <b>ASSISTANT:</b> [ANSWER]
3D Instance Segmentation	<b>USER:</b> Given the 3D scene, please segment the [CATEGORY]. <b>ASSISTANT:</b> [ANSWER] <b>USER:</b> Please segment the [CATEGORY] in this 3D scene. <b>ASSISTANT:</b> [ANSWER]
3D Scene Caption	<b>USER:</b> Please describe the 3D scene. <b>ASSISTANT:</b> [ANSWER]
3D Referring Segmentation	<b>USER:</b> Given the 3D scene, please segment this object: [DESCRIPTION]. <b>ASSISTANT:</b> [ANSWER] <b>USER:</b> Following are descriptions of an object: [DESCRIPTION]. <b>ASSISTANT:</b> [ANSWER]

Table 7. Data formulation for general pre-training.

**Spatial Relation Reasoning:**

**Step 1:**

**Question Answering Task and Reasoning Segmentation Task:**

- **USER:** Given the 3D scene, [QUESTION]. Please segment the question-related objects. **ASSISTANT:** [ANSWER]
- **USER:** [QUESTION] Please segment the question-relevant objects. **ASSISTANT:** [ANSWER]
- **USER:** Please segment the relevant objects for the question: [QUESTION]. **ASSISTANT:** [ANSWER]

**Referring Task:**

- **USER:** Please segment the relevant objects for this description: [DESCRIPTION]. **ASSISTANT:** [ANSWER]
- **USER:** This is a description of an object: [DESCRIPTION]. Please segment the description-related objects. **ASSISTANT:** [ANSWER]
- **USER:** Which objects related to this description: [DESCRIPTION]? Please segment it. **ASSISTANT:** [ANSWER]

---

**Step 2:**

**Question Answering Task:**

- **USER:** Given the 3D scene, [QUESTION]. Please answer the question. The question-related objects are [SEG]...[SEG]. You may need to pay attention to them. **ASSISTANT:** [ANSWER]
- **USER:** Answer this question: [QUESTION]. The question-relevant objects are [SEG]...[SEG]. You should pay attention to them. **ASSISTANT:** [ANSWER]

**Reasoning Segmentation Task:**

- **USER:** Given the 3D scene, [QUESTION]. Please answer the question with segmentation mask. The question-related objects are [SEG]...[SEG]. You may need to pay attention to them. **ASSISTANT:** [ANSWER]
- **USER:** Answer this question and output segmentation mask: [QUESTION]. The question-relevant objects are [SEG]...[SEG]. You should pay attention to them. **ASSISTANT:** [ANSWER]

**Referring Task:**

- **USER:** This is a description of an object: [DESCRIPTION]. Please segment this object. The description-related objects are [SEG]...[SEG]. You may need to pay attention to them. **ASSISTANT:** [ANSWER]
- **USER:** Please segment the object match to this description: [DESCRIPTION]. The description-relevant objects are [SEG]...[SEG]. You should pay attention to them. **ASSISTANT:** [ANSWER]

Figure 11. More template for Relevant Reasoning Segmentation.

**Mask Decoder.** The mask decoder is also derived from the pre-trained OneFormer3D [25] model, featuring a 6-layer transformer decoder with a feature dimension of 256. We substitute the default queries with our designated [SEG] token for decoding the segmentation masks.

**Visual-Language Connector.** We employ QFormer [29] as the visual-language connector to condense dense point cloud features into adaptable latent queries. The architecture consists of a 6-layer QFormer with a 768-dimensional feature space, initialized with pre-trained word and positional embeddings from BERT [13]. The model maintains a vocabulary size of 30,522 and 512 position embeddings.

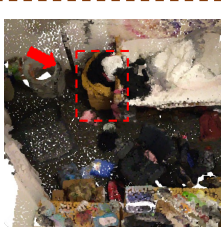
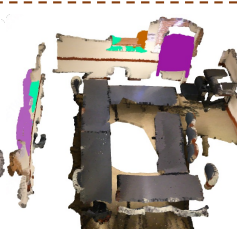
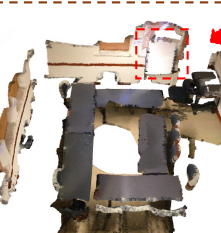
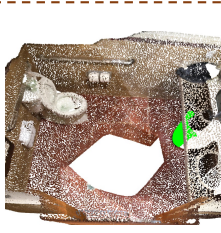
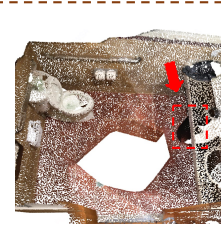
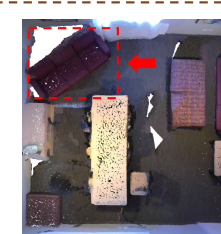
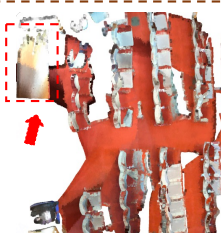
Instruction	Prediction	Relevant Objects	Ground Truth
<p><b>USER:</b> What is the object that is used for sitting and located in the living room, near the tv and the coffee table?</p>			
<p><b>USER:</b> What is the largest piece of furniture designed for sitting, next to the desk?</p>			
<p><b>USER:</b> What is the object that is used for writing notes and is located near the window?</p>			
<p><b>USER:</b> What is the object that is used for disposing of waste and is located near the counter?</p>			
<p><b>USER:</b> What is the largest piece of furniture designed for sitting, next to the coffee table?</p>			
<p><b>USER:</b> What is the largest piece of furniture designed for sitting, next to the coffee table?</p>			

Figure 12. More qualitative results on 3D ReasonSeg.

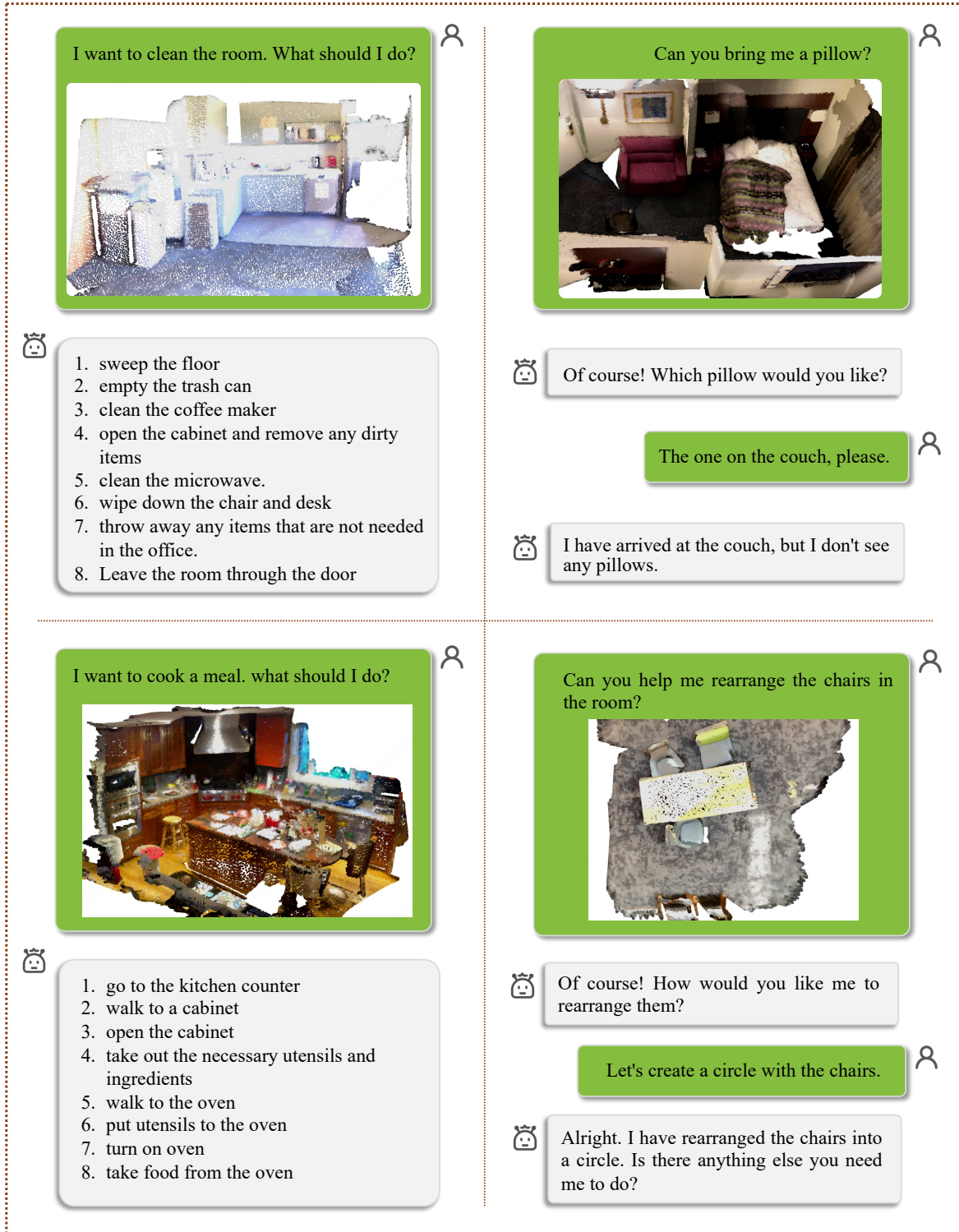


Figure 13. More qualitative results on scene description and embodied planning.